2019-01-0014 Published 15 Jan 2019

Heat of Vaporization and Species Evolution during Gasoline Evaporation Measured by DSC/TGA/MS for Blends of C1 to C4 Alcohols in Commercial Gasoline Blendstocks

Gina M. Fioroni, Earl Christensen, Lisa Fouts, and Robert McCormick National Renewable Energy Laboratory

Citation: Fioroni, G.M., Christensen, E., Fouts, L., and McCormick, R., "Heat of Vaporization and Species Evolution during Gasoline Evaporation Measured by DSC/TGA/MS for Blends of C1 to C4 Alcohols in Commercial Gasoline Blendstocks," SAE Technical Paper 2019-01-0014, 2019, doi:10.4271/2019-01-0014.

Abstract

Evaporative cooling of the fuel-air charge by fuel evaporation is an important feature of direct-injection spark-ignition engines that improves fuel knock resistance and reduces pumping losses at intermediate load, but in some cases, may increase fine particle emissions. We have reported on experimental approaches for measuring both total heat of vaporization and examination of the evaporative heat effect as a function of fraction evaporated for gasolines and ethanol blends. In this paper, we extend this work to include other low-molecular-weight alcohols and present results on species evolution during fuel evaporation by coupling a mass spectrometer to our differential scanning calorimetry/thermogravimetric analysis instrument. The alcohols examined were methanol, ethanol, 1-propanol, isopropanol, 2-butanol, and isobutanol at 10 volume percent, 20 volume percent, and 30 volume percent. The results show that total heat of vaporization of the alcohol gasoline blends is in line with the decreasing heat of vaporization in kilojoules per kilogram with increasing alcohol carbon number, as expected. Mass spectrometer results show that methanol fully evaporates at significantly lower fraction evaporated relative to other alcohols even though it is present at higher molar concentration at a fixed volumetric concentration. Certain alcohols, especially methanol and ethanol, can suppress the evaporation of aromatic compounds such as cumene during the evaporation process in some samples. While the use of mass spectrometry to analyze the composition of the evolving gas mixture provided useful results for a relatively simple research gasoline (FACE B), additional research is required to practically apply this methodology to more complex commercial gasolines.

Introduction

To reduce greenhouse gas emissions and improve fuel economy in the light-duty transportation sector, research has focused on increasing spark ignition (SI) engine efficiency [1]. This can be accomplished by several methods, which include: turbocharging, direct injection (DI), increasing compression ratio, down-speeding, and downsizing; however, most of these strategies tend to increase in-cylinder pressure and temperature [2, 3, 4]. The increase in pressure and temperature can require fuels with higher knock resistance, especially if these strategies are to be pursued aggressively. This can be circumvented in part using DI of the fuel, which results in evaporative cooling of the air-fuel mixture and which increases effective knock resistance, potentially by as much as five research octane number units [5]. Evaporative cooling also reduces heat transfer and increases specific heat ratio, resulting in improved efficiency at intermediate loads [6, 7]. The addition of alcohols to the fuel can further increase the evaporative cooling effect due to their high heat of vaporization (HOV) further exploiting the benefits of this strategy [4].

Alcohols can have a much higher HOV than typical gasoline hydrocarbons. For example, the HOV of methanol is about four times higher and ethanol is about three times higher than that of typical gasoline hydrocarbons [8]. Table 1 lists the HOV values reported at 298.15K [9] and boiling points of some alcohols of interest that were examined in this study.

Several studies have observed increased particulate matter (PM) emissions for ethanol blends relative to the base hydrocarbon gasoline or other hydrocarbon fuels [11, 12, 13,

TABLE 1 Heat of vaporization and boiling point of various alcohols

Alcohol	HOV (kJ/kg) [9]	Boiling Point (°C) [10]
Methanol	1173.5	65
Ethanol	918.6	78
1-Propanol	788.7	97
Isopropanol	743.8	83
Isobutanol	685.4	108
2-Butanol	670.5	100

Created by the National Renewable Energy Laboratory

14, 15, 16]. These studies have suggested that increased evaporative cooling from the presence of ethanol causes high boiling point aromatic compounds, which are largely responsible for PM formation, to be resistant to evaporation and mixing with air and thus much more likely to form PM. This effect is thought to be particularly relevant when the fuel spray impinges on the top of the piston or cylinder wall [12, 14, 17, 18]. The impact of alcohols other than ethanol on PM formation has not been widely studied.

Because HOV is a key fuel property, there has been interest in measurement of the HOV of gasoline and gasoline-alcohol blends. Application of classical methods of measuring the HOV of complex mixtures using the Clausius-Clapeyron equation have not been successful [19, 20]. We have worked to develop a differential scanning calorimetry (DSC)/thermogravimetric analysis instrument (TGA) method to measure total HOV of gasoline-ethanol blends [8]. The initial method suffered from sample loss prior to starting the experiment during sample handling. We were able to further develop the method to limit initial sample loss [21] and extend the method to examine enthalpy evolution during evaporation of gasoline-ethanol blends. During this research, it was noted that there was a distinct increase in evaporative cooling of the mixture during the evolution of ethanol from a research gasoline blend. The heat flow then dropped back down to that of the base fuel once the ethanol had finished evaporating. This increased cooling effect was extended as higher volumes of ethanol were blended. For a more complex surrogate fuel containing a high percentage of aromatics (35 volume percent (vol.-%)), the enthalpy evolution was not as clear or as defined. We attributed this to the formation of a series of azeotropes between ethanol and the aromatics in the fuel. To better understand these phenomena, a high-resolution mass spectrometer (MS) was coupled to our current DSC/TGA instrument to allow monitoring of distinct components of the fuel.

This current work focuses on answering the question of how fuel composition impacts enthalpy and species evolution during evaporation of gasoline and gasoline-alcohol blends using the newly developed DSC/TGA/MS method. The goal of this work was to examine the evolution of alcohol and aromatic components in both a surrogate fuel as well as in two commercial-grade gasoline blendstock samples. Additionally, the impact of other alcohols in the C1 to C4 range was compared to ethanol.

Methods

Fuels

Gasoline blendstocks were obtained from petroleum refiners and include a wintertime conventional blendstock for oxygenate blending (CBOB) and a summertime reformulated blendstock for oxygenate blending (RBOB). A reference gasoline FACE (Fuels for Advanced Combustion Engines) B [22] was utilized to examine the impact of alcohols on the evaporation of the aromatic compound, cumene. Pure component alcohols and cumene were purchased from Sigma Aldrich in 99% purity or greater. Table 2 contains properties of these materials, including summary results of detailed hydrocarbon analysis (DHA). The aromatic compounds in FACE B consist almost entirely of xylenes and ethyl benzene.

TABLE 2 RBOB, CBOB, and FACE B fuel properties

Property	RBOB	CBOB	FACE B
Research octane number	87.5	86.8	95.8
Motor octane number	80.6	81.1	92.4
Density (g/cm^3)	0.7438	0.7078	0.6970
Reid vapor pressure (kPa)	36.40	80.05	50.3
HOV (DSC/TGA) (kJ/kg)	359	358	341
DHA (vol.-%)			
n-Paraffins	11.6	23.2	8.0
i-Paraffins	40.9	41.6	86.9
Cycloparaffins	6.0	7.1	0.1
Aromatics	33.7	20.4	5.8
Olefins	7.06	7.5	0.02

Blending

All samples were prepared by hand blending by volume. Prior to blending, the base fuel was stored in the freezer overnight to avoid evaporation of the light end of the fuel. Once the blends were prepared, the samples were immediately capped in air-tight aluminum cans and stored in the freezer. The weight of the blend component and the base fuel were recorded during the blending process. The blend level was validated by gas chromatography using a modified version of ASTM International (ASTM) method D5501 for all blends prepared in CBOB and RBOB. The blend level validation results are included in Table A.1 in the appendix and show that blends were prepared accurately and were within +/- 2% of the intended volume percentage. Blends were prepared at 10 vol.-%, 20 vol.-%, and 30 vol.-%. Methanol was blended into the RBOB, but not the CBOB. Distillation was performed by ASTM D86, total HOV was calculated from the DHA of each sample [8], and the Reid vapor pressure (RVP) as dry vapor pressure equivalent (ASTM D5191) was measured in-house using an Eralytics vapor pressure tester, ERAVAP.

Samples of FACE B with 20% cumene and 30% of each alcohol were also prepared by hand blending. Because the volume required for DSC/TGA/MS is very small, only small laboratory size samples (10 mL) of these blends were prepared, and the blend level accuracy was not determined. Cumene is a nine-carbon aromatic compound, and several studies have shown that C9 and larger aromatics are primarily responsible for PM emissions from DISI engines [23, 24]. Cumene (boiling point 153°C) is also volatile enough to evaporate at room temperature, the conditions used in this study [18]. All samples were analyzed utilizing the new DSC/TGA/MS method to track species and enthalpy evolution throughout the entire evaporation process.

DSC/TGA/MS

A Q600 series DSC/TGA from TA Instruments (New Castle, DE) was coupled to a JOEL JMS-GC Mate II high-resolution

MS (Peabody, MA). Both instruments were calibrated per the manufacturer's specification prior to analysis. Care was taken to open sample containers minimally to avoid evaporation of the light ends of the sample. For analysis, an aliquot of sample was transferred to a tared platinum DSC/TGA pan (TA part# 960149.901) using a gas-tight syringe and a nominal sample volume of 20 µL. The sample was transferred directly into the tared pan inside the instrument, the furnace door was closed, and the experiment was started. The experiment was conducted at ambient laboratory conditions (20°C-22°C). Upon initiation of the experiment, the nitrogen purge gas in the furnace was switched from 5 mL/min to 50 mL/min after 0.1 min to aid with sample evaporation and transport evaporated species to the MS. The DSC/TGA instrument was used to track the enthalpy change as heat flow from the sample (when compared to a reference pan) while a heated transfer line (100°C) continually sampled from the TGA furnace directly into the orifice of the high-resolution MS. The MS was set to scan from mass/charge (m/z) 33-200 to avoid ions 28 and 32 that are associated with nitrogen (purge gas used in DSC/TGA) and oxygen (introduced from the ambient air when the sample furnace is opened). In the case of methanol and 1-propanol, the MS scan range was 31-200, as ion 31 was necessary to monitor the evolution of these two alcohols. For each compound monitored, we chose a specific ion that was used to track the evolution of the species of interest. Table A.2 in the appendix contains a list of ions used for monitoring each alcohol. For the alcohols, we chose the largest ion visible that was unique from those ions present in the base fuels.

For the less complex composition of the FACE B research gasoline, identification of which ion corresponds to which compound was straightforward. For the more complex CBOB and RBOB samples, ions cannot be individually assigned to a compound due to the large number of compounds that share the same ion; therefore, ions were grouped by the class of compounds they represent. Table 2 lists the DHA summary analysis for each fuel showing that the major composition of both fuels was n-paraffins, isoparaffins, and aromatics, which made up 75% and 85% of the sample, respectively. From the MS, ions 43, 57, 71, and 85 represent the paraffin and isoparaffin portion of the sample. Ion 105 represents the C8 aromatic potion of the sample, and ion 120 represents the C9 aromatic portion of the sample.

Results

FACE B Blends DSC/TGA/MS

Table 3 lists the HOV at 25°C of the blends in FACE B as calculated from DHA. The alcohols are listed in order from the highest to the lowest pure component HOV. The trend in HOV of the blend is as expected and follows with the pure component HOV.

Figure 1 shows results of MS analysis of species evolving during evaporation of FACE B-20% cumene-30% alcohol blends. The total ion current (TIC) was tracked along with isooctane, cumene, xylenes plus ethyl benzene (labelled as xylenes for simplicity), and the main ion for the alcohol of interest. Note that TIC is unitless, therefore the Y axis labels in the figures do not have unit labels. The fraction of sample evaporated was calculated by dividing the cumulative sum of the TIC at a given fraction evaporated by the total sum of the TIC. For simplicity, samples were adjusted to be on a scale of 0 to 1.0, with 0 being the start of sample evaporation and 1.0 being complete sample evaporation. Cumene evolution was exclusively tracked using ion 120.

TABLE 3 HOV values calculated by DHA for FACE B blends with 20% cumene and 30% alcohol.

30% Alcohol in FACE B	HOV (kJ/kg)
A0 (FACE B + 20% Cumene)	335.6
Methanol	656.6
Ethanol	560.9
1-Propanol	508.4
Isopropanol	495.0
Isobutanol	470.0
2-Butanol	463.8

Created by the National Renewable Energy Laboratory

In the graphs in Figure 1, it can be noted that methanol evaporates very early in the sample evaporation process-all the methanol had evaporated by the time 30% of the total sample had evaporated. Ethanol and isopropanol evaporate by the time 60% of the sample evaporated, double that of methanol. On the other hand, 1-propanol and 2-butanol take even longer and evaporate at 80% or higher of sample evaporated while isobutanol takes the longest to completely evaporate from the sample and remains until over 90% of the sample has evaporated. The lower-molecular-weight, lower-boiling-point alcohols (methanol and ethanol) evaporate off at a lower fraction evaporated even though they are at a higher molar concentration due to their lower molecular weight. Also, of interest is that the addition of alcohol to the sample causes a sharper drop in cumene concentration at the termination of the paraffin and isoparaffin portion of the sample evaporating (FACE B is composed of 87% isoparaffin) when compared to the A0 (no alcohol) case. This occurs after the alcohol is fully evaporated in most cases and may indicate the completion of evaporation of an azeotrope of cumene with other fuel components.

In Figure 2a and 2b (expanded region of Figure 2a), the fraction of cumene remaining in the sample was plotted against the fraction evaporated for all the FACE B blends with cumene and alcohols. Cumene has a higher fraction remaining for methanol, ethanol, and the propanol isomers throughout the evaporation process relative to A0 (FACE B + 20% Cumene) and the butanol isomers. Ethanol shows the highest cumene levels in the 50%-80% evaporated range. Methanol showed a slight increase in cumene remaining in the 20%-40% region, which coincides with the termination of its evaporation from the sample in the 25%-30% range (Figure 1). There is also an elevated amount of cumene remaining for 1-propanol and isopropanol in the 60%-80% fraction evaporated range, although not as pronounced as was observed for ethanol. For the least volatile alcohols, 2-butanol and isobutanol, the cumene remaining essentially overlays the A0 case.

FIGURE 1 Results of mass spectral analysis during evaporation of FACE B blends with cumene (20 vol.-%) and various alcohols (30 vol.-%).

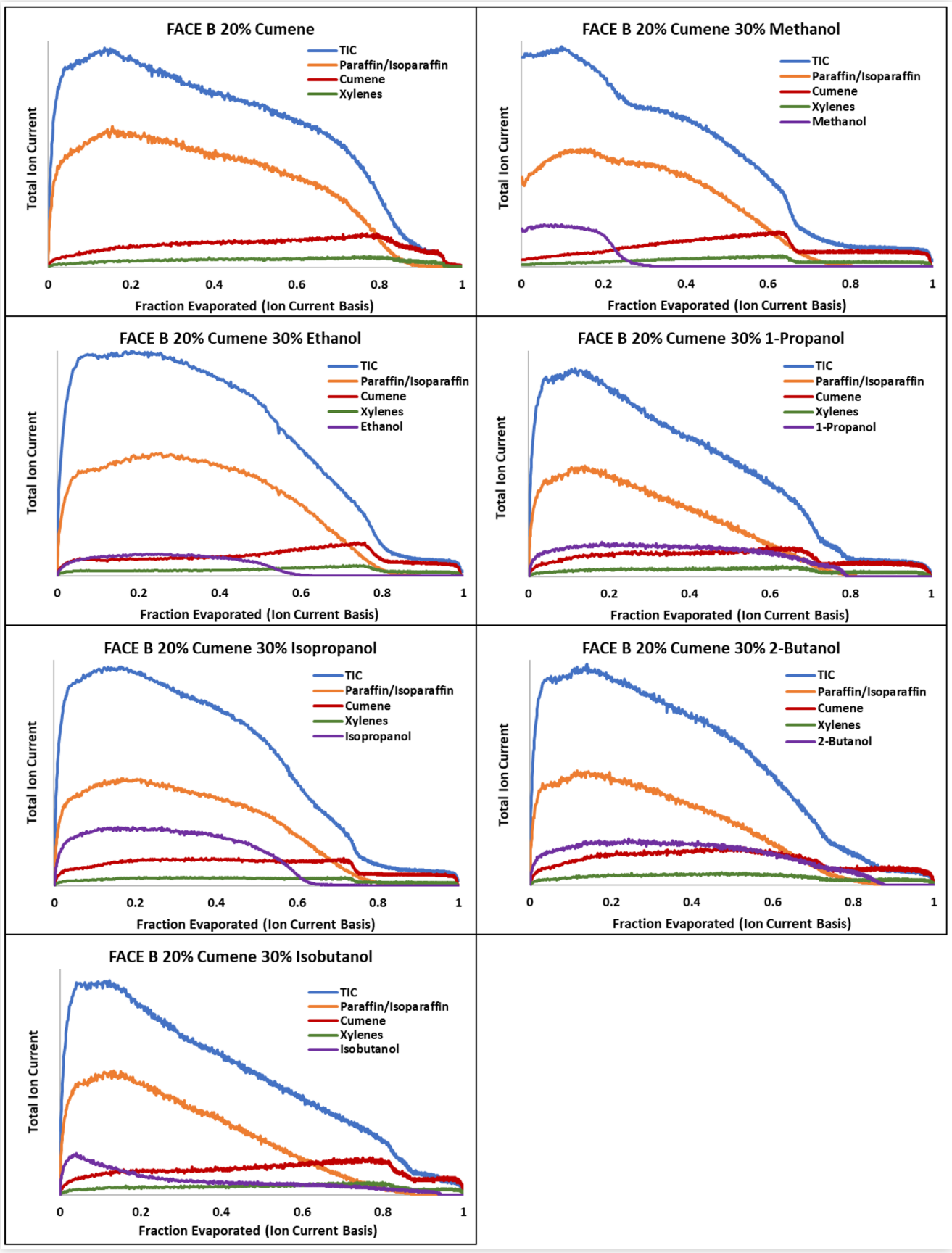

Created by the National Renewable Energy Laboratory

FIGURE 2 Cumene fraction remaining versus fraction of sample evaporated for 30% alcohol blends in FACE B research gasoline.

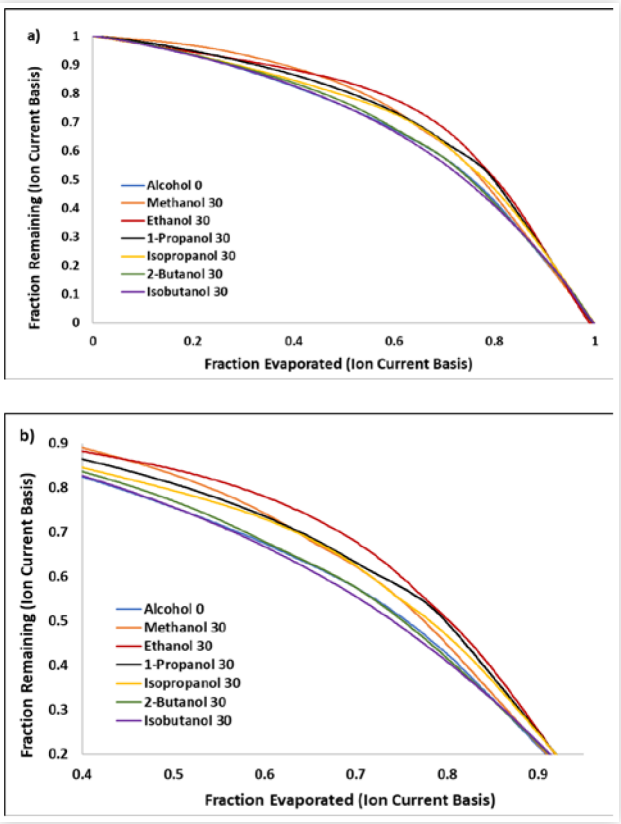

Created by the National Renewable Energy Laboratory

FIGURE 3 RVP for alcohol blends with a) RBOB and b) CBOB.

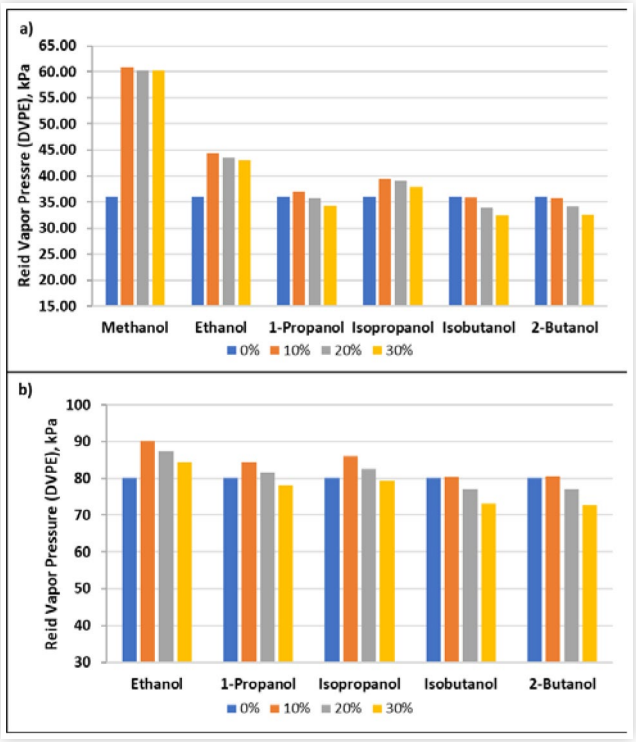

Created by the National Renewable Energy Laboratory

Alcohol Blends with RBOB and CBOB

Figure 3 shows the results for the RVP of the alcohol blends with CBOB and RBOB. RVP and HOV data are included in Table A.3 in the appendix. Methanol and ethanol increased RVP significantly, a well-known effect [25]. Isopropanol also increased RVP, especially in the low-vapor-pressure RBOB. The effect of 1-propanol was marginal, while 2-butanol and isobutanol showed reductions in the RVP. Figure 4 shows D86 data for the 30% blends with CBOB and RBOB. Figure A.1 in the appendix plots D86 data for all blend levels. As expected, there is a depression in the distillation curves from the addition of the alcohols. Methanol, ethanol, and isopropanol show the greatest impact on boiling point depression while 2-butanol, isobutanol, and 1-propanol all show a similar depression in the curve in both RBOB and CBOB. Methanol, which has the lowest boiling point (65°C), has the largest effect, while ethanol and isopropanol, which have similar boiling points (78°C and 83°C, respectively), show the next largest effect. 1-propanol and 2-butanol, which have boiling points of around 100°C, and isobutanol, with a boiling point of 108°C, show the smallest depressions in the distillation curve when compared to methanol, ethanol, and isopropanol.

Figure 5 shows the total HOV calculated by DHA for the RBOB and CBOB blends. These charts show the blends in order, from left to right, of alcohol HOV (methanol being the

FIGURE 4 D86 distillation curves for 30% alcohol blends with a) RBOB and b) CBOB.

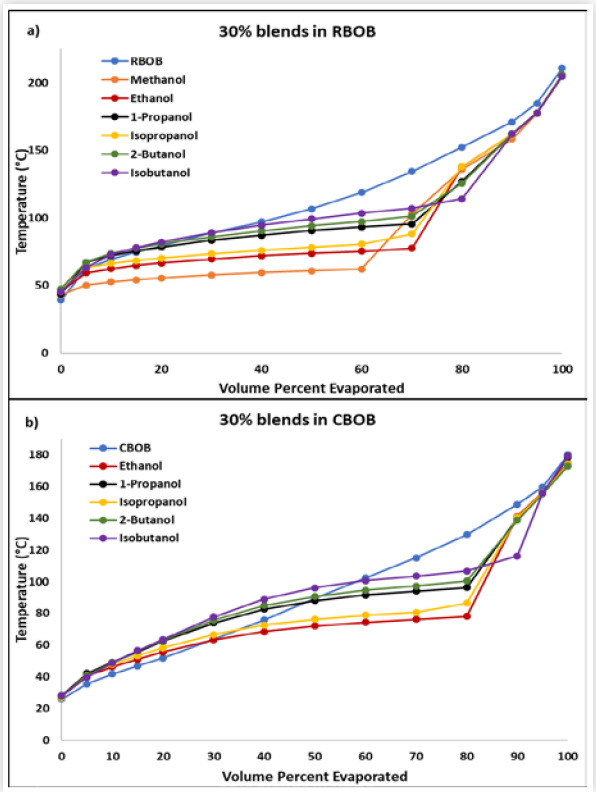

Created by the National Renewable Energy Laboratory

FIGURE 5 Total HOV for a) RBOB and b) CBOB blends.

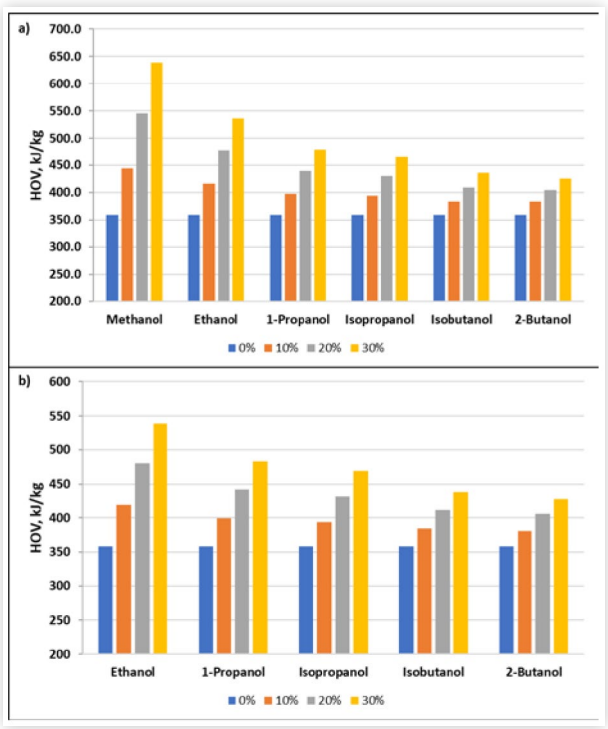

highest and 2-butanol being the lowest). Trends are as expected with alcohol HOV and blend level. Blending of 30 vol.-% methanol increases the HOV by over 80%, ethanol increases HOV by almost 50%, while blending of 2-butanol, the component with the lowest HOV, increases HOV by only 19%.

Figure 6 shows the heat flow curves from the DSC/TGA for the various alcohols blended into RBOB at 30 vol.-%. The relative magnitude of the heat flow is primarily affected by the evaporation rate as well as the HOV. In this experiment with open pans the evaporation rate is likely roughly proportional to the vapor pressure [21]. The methanol blend shows the greatest heat effect, followed by ethanol and then isopropanol - in line with expectations. A key feature of the heat flow curves is the fraction evaporated where the alcohol heat effect ends. For these A30 blends, the methanol appears to

FIGURE 6 DSC/TGA heat flow curves for 30% alcohols in RBOB.

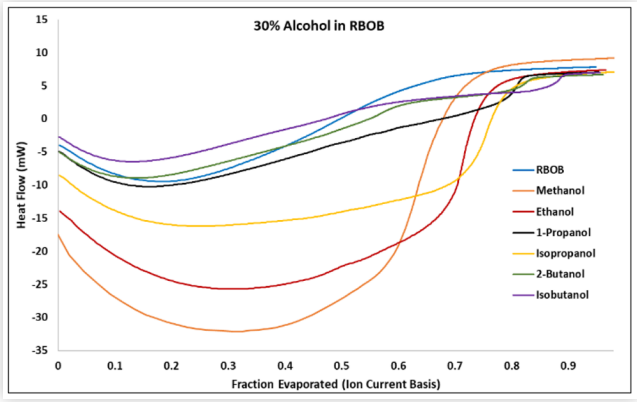

be completely evaporated at 60%; the ethanol at 75%; 1-propanol, isopropanol, and 2-butanol at 80%; and isobutanol at 90%. Qualitative comparison of where the heat effect ends and where the alcohol finishes evaporating (as determined from the MS) yields reasonable agreement for all samples (not shown).

Mass spectral data for 10% blends of alcohols in RBOB are shown in Figure 7. As noted in the Methods section, due to the complex nature of the RBOB sample, it was not possible to relate specific compounds to a specific ion in the mass spectrum. Instead, ions were grouped together to represent the paraffin/isoparaffin, C8 aromatic, and C9 aromatic portions of the sample. The TIC was re-scaled by half for all samples.

Examination of the 10% blend MS analysis results in Figure 7 shows that methanol is all evaporated by 30% total sample evaporated and ethanol is all evaporated by 45% total sample evaporated. The propanols are fully evaporated between 50% and 60%, while isobutanol and 2-butanol are fully evaporated between 70% and 80%. For the alkanes, there does not seem to be much difference between the base RBOB and the alcohol blends despite the known azeotropes formed with alcohols and paraffins [26, 27, 28]. A possible exception is 1-propanol, where the alkanes appear to be completely evaporated at significantly lower total fraction evaporated than for any of the other blends. The aromatics curves all show a first phase evaporation with a dip to a second phase evaporation at a lower level. This occurs at 50% for A0, just over 60% for ethanol, 55% for 1-propanol, and 70% for isopropanol and isobutanol.

Figure 8 shows evolving gas compositions for the 30% blend level for the RBOB samples. As would be expected, the addition of more alcohol extends the evaporation of the alcohol to a higher fraction evaporated. Methanol remains in the sample until 55% of the sample has evaporated, ethanol remains in the sample until about 70% has evaporated versus 45% evaporated for the 10% blend cases. The propanols are extended to between 70% and 80%, and the isobutanol appears to extend out to about 90% evaporated. 2-butanol presents an unusual evaporation profile at this high blend level with two stages of evaporation ending at nearly 90% of the total sample evaporated. These values are in good agreement with similar results from the heat flow curves (Figure 6) as noted previously. The aromatics behave similarly to the 10% blend case, exhibiting a first phase evaporation that corresponds to near the termination of alkane evaporation at about 70% for the ethanol and 1-propanol blends, almost 80% for isopropanol, and perhaps past 80% for isobutanol.

Figure 9 shows results for the 10% blends of alcohols (A10) with CBOB. At the 10% blend level, ethanol finished evaporating at a similar percent evaporated (45%) as for the RBOB. However, in the case of the propanols, in CBOB, they finished evaporating later in the 60%-70% range rather than 50%-60% as for the RBOB. The isobutanol and 2-butanol also remained to higher percent evaporated at about 90% evaporated versus 80% for RBOB. This is likely due to CBOB containing fewer heavy and higher boiling components than the RBOB. Note that the T90 of CBOB was 150°C while the T90 of the RBOB was 170°C.

FIGURE 7 Results of mass spectral analysis during evaporation for RBOB and blends of 10% alcohols with RBOB.

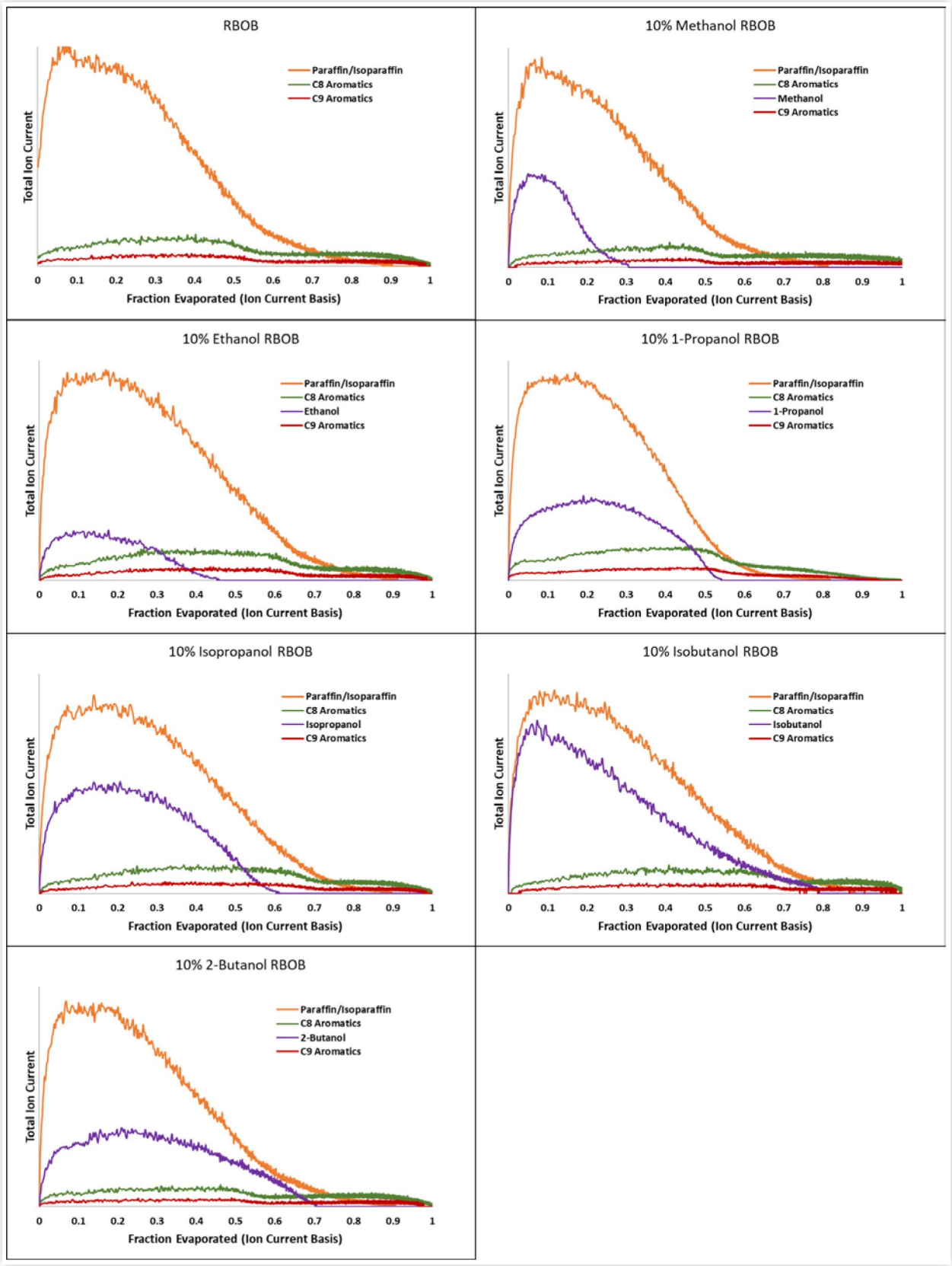

Created by the National Renewable Energy Laboratory

FIGURE 8 Results of mass spectral analysis during evaporation for RBOB and A30 blends with RBOB

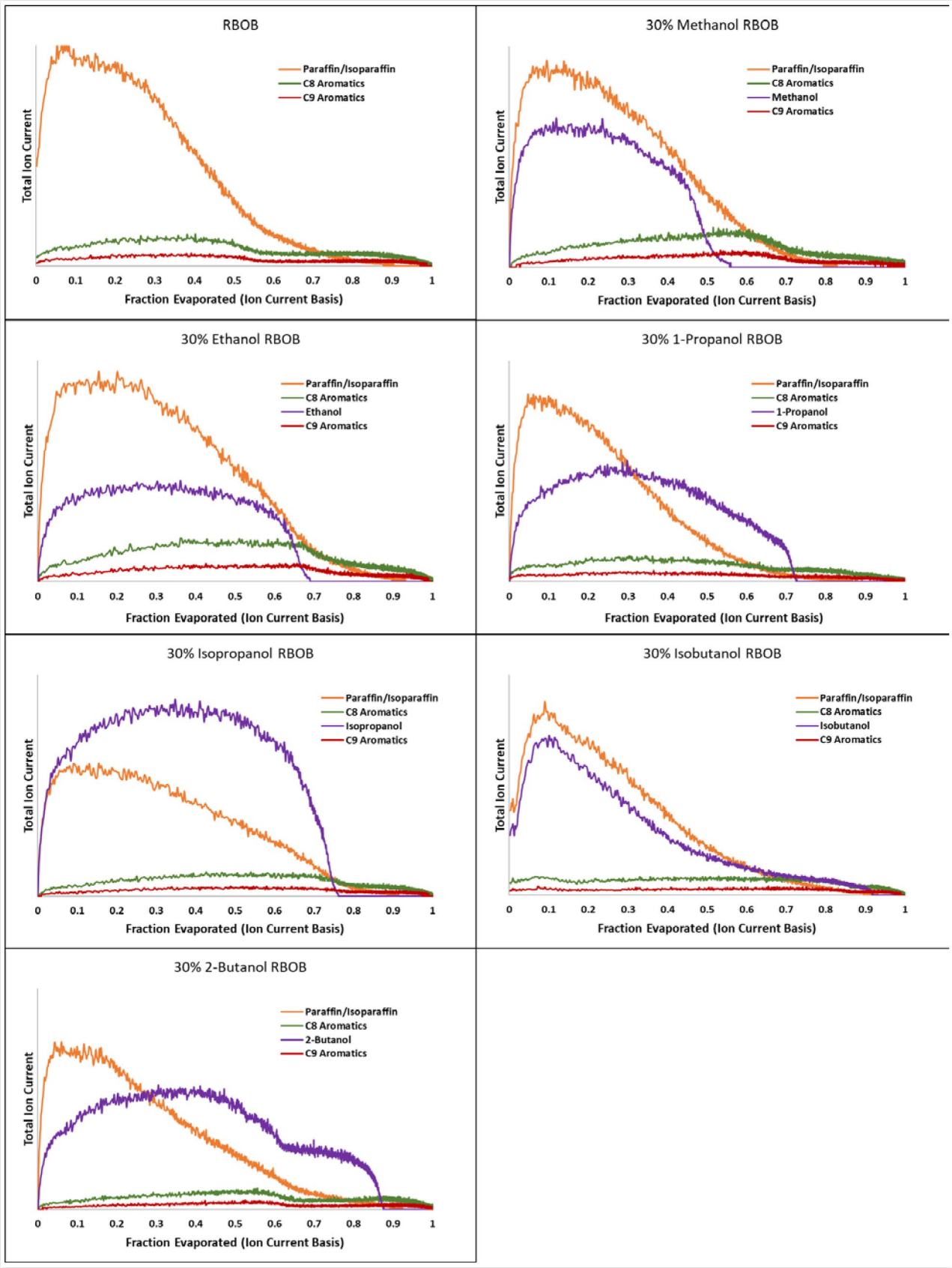

Created by the National Renewable Energy Laboratory

FIGURE 9 Results of mass spectral analysis during evaporation for CBOB and A10 blends with RBOB.

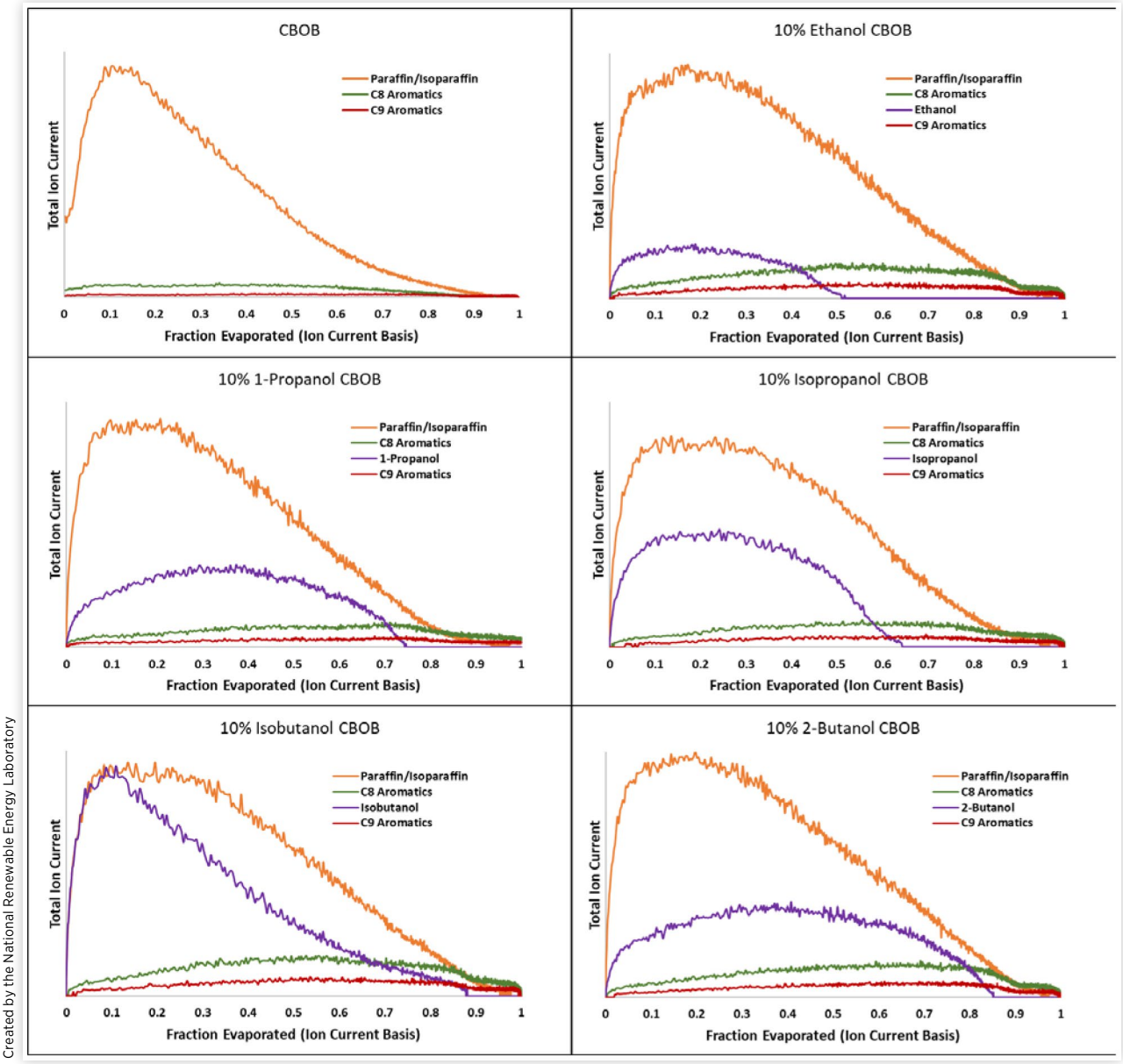

Summary/Conclusions

In the relatively simple research gasoline FACE B, the evaporation behavior of cumene blends with various alcohols was easily observed. The lower the boiling point and the smaller the alcohol chain, the more rapid evaporation of the alcohol from the sample. Methanol was completely evaporated by 30% fraction evaporated, ethanol and isopropanol were similar at 60% fraction evaporated, and 2-butanol took the longest at 80% or higher percent fraction evaporated. Evaporation of cumene was delayed by the presence of methanol, ethanol, or the propanol isomers but unaffected by the butanol isomers. This effect of delaying aromatic compound evaporation has been reported previously for ethanol blends [18, 29, 30]. This is caused by the combined effect of the lower boiling point of the alcohols such that they must evaporate first and non-ideal vapor-liquid equilibrium effects for blends of these alcohols into gasoline [29]. Non-ideal solution (not according to Raoult's law) vapor-liquid equilibrium is amply demonstrated for the C1 to C3 alcohols by their impact on Reid vapor pressure and the distillation curve as well. The delay of aromatic evaporation by vapor-liquid equilibrium effects may be equally important as evaporative cooling in causing increased particulate matter emissions from alcohol blends under some conditions [18].

The effects on Reid vapor pressure and distillation in FACE B were also observed in blends of the alcohols in conventional blendstock for oxygenate blending and reformulated blendstock for oxygenate blending. The C1 to C3 alcohols acted to increase Reid vapor pressure and significantly depress the distillation curve while C4 alcohols decreased Reid vapor pressure and had a much smaller effect on distillation. Effects of the alcohols on aromatic compound evaporation were more

difficult to discern in these complex full boiling range gasoline blendstocks because of the large number of aromatic (and other) compounds present. With additional development of the differential scanning calorimetry/thermogravimetric analysis/mass spectrometry method it may prove possible to quantitatively examine evaporation of specific carbon number compounds within compound classes, especially C9 and larger aromatics, but this is out of reach using the current experimental and data analysis approach.

In observing the evaporative cooling heat effect from the sample using the differential scanning calorimetry/thermogravimetric analysis, methanol, ethanol, and isopropanol showed the largest heat flow. Extension of the differential scanning calorimetry/thermogravimetric analysis/mass spectrometry concept to real-world conventional blendstock for oxygenate blending and reformulated blendstock for oxygenate blending samples showed several interesting results with some different observations than were noted for the simpler FACE B case. For all alcohol blends, there was a relatively sharp drop in heat flow when the alcohol was fully evaporated. There was good agreement between the heat flow curves and the mass spectrometry data on the fraction evaporated where alcohol evaporation was complete.

For all samples, the species evaporation profiles appeared strongly affected by interactions between the alcohols and hydrocarbon gasoline components. One avenue of future development of this experiment will be to examine specific azeotropic interactions using model systems consisting of an alcohol and a single hydrocarbon component or a small number of hydrocarbon components. Experiments could examine evaporation of systems exhibiting a series of azeotropes with similar compounds or multiple azeotropic interactions with compounds of different classes.

References

1. U.S. Environmental Protection Agency, Office of Transportation and Air Quality, "EPA and NHTSA Set Standards to Reduce Greenhouse Gases and Improve Fuel Economy for Model Years 2017-2025 Cars and Light Trucks. [S.l.]," EPA-420-F-12-051, August 2012, https://nepis.epa.gov/Exe/ZyPDF.cgi/P100EZ7C.PDF?Dockey=P100EZ7C.PDF.
2. Kasseris, E. and Heywood, J., "Charge Cooling Effects on Knock Limits in SI DI Engines Using Gasoline/Ethanol Blends: Part 2-Effective Octane Numbers," *SAE Int. J. Fuels Lubr.* 5(2):844-854, 2012, doi:10.4271/2012-01-1284.
3. Kasseris, E. and Heywood, J., "Charge Cooling Effects on Knock Limits in SI DI Engines Using Gasoline/Ethanol Blends: Part 1-Quantifying Charge Cooling," SAE Technical Paper 2012-01-1275, 2012, doi:10.4271/2012-01-1275.
4. Ratcliff, M., Burton, J., Sindler, P., Christensen, E. et al., "Effects of Heat of Vaporization and Octane Sensitivity on Knock-Limited Spark Ignition Engine Performance," SAE Technical Paper 2018-01-0218, 2018, doi:10.4271/2018-01-0218.
5. Chow, E., Heywood, J., and Speth, R., "Benefits of a Higher Octane Standard Gasoline for the U.S. Light-Duty Vehicle Fleet," SAE Technical Paper 2014-01-1961, 2014, doi:10.4271/2014-01-1961.
6. Wyszynski, L., Stone, C., and Kalghatgi, G., "The Volumetric Efficiency of Direct and Port Injection Gasoline Engines with Different Fuels," SAE Technical Paper 2002-01-0839, 2002, doi:10.4271/2002-01-0839.
7. Jung, H., Shelby, M., Newman, C., and Stein, R., "Effect of Ethanol on Part Load Thermal Efficiency and CO_2 Emissions of SI Engines," *SAE Int. J. Engines* 6(1):456-469, 2013, doi:10.4271/2013-01-1634.
8. Chupka, G., Christensen, E., Fouts, L., Alleman, T. et al., "Heat of Vaporization Measurements for Ethanol Blends up to 50 Volume Percent in Several Hydrocarbon Blendstocks and Implications for Knock in SI Engines," *SAE Int. J. Fuels Lubr.* 8(2):251-263, 2015, doi:10.4271/2015-01-0763.
9. Chickos, J.S. and Acree, W.E. Jr., "Enthalpies of Vaporization of Organic and Organometallic Compounds, 1880-2002," *J. Phys. Chem. Ref. Data* 32:519-878, 2003, doi:10.1063/1.1529214.
10. Shen, V.K., Siderius, D.W., Krekelberg, W.P., and Hatch, H.W., *NIST Standard Reference Simulation Website, NIST Standard Reference Database*, One Seventy Third Edition, (National Institute of Standards and Technology: Gaithersburg MD), 20899.
11. Chen, L., Braisher, M., Crossley, A., Stone, R. et al., "The Influence of Ethanol Blends on Particulate Matter Emissions from Gasoline Direct Injection Engines," SAE Technical Paper 2010-01-0793, 2010, doi:10.4271/2010-01-0793.
12. Chen, Y., Zhang, Y., and Cheng, W., "Effects of Ethanol Evaporative Cooling on Particulate Number Emissions in GDI Engines," SAE Technical Paper 2018-01-0360, 2018, doi:10.4271/2018-01-0360.
13. Butler, A., Sobotowski, R., Hoffman, G., and Machiele, P., "Influence of Fuel PM Index and Ethanol Content on Particulate Emissions from Light-Duty Gasoline Vehicles," SAE Technical Paper 2015-01-1072, 2015, doi:10.4271/2015-01-1072.
14. He, X., Ratcliff, M.A., and Zigler, B.T., "Effects of Gasoline Direct Injection Engine Operating Parameters on Particle Number Emissions," *Energy & Fuels* 26(4):2014-2027, 2012, doi:10.1021/ef201917p.
15. Storch, M., Koegl, M., Altenhoff, M., Will, S. et al., "Investigation of Soot Formation of Spark-Ignited Ethanol-Blended Gasoline Sprays with Singe- and Multi-Component Base Fuels," *Applied Energy* 181:278-287, 2016, doi:10.1016/j.apenergy.2016.08.059.
16. Vuk, C. and Vander Griend, S.J., "Fuel Property Effects on Particulates in Spark Ignition Engines," SAE Technical Paper 2013-01-1124, 2013, doi:10.4271/2013-01-1124.
17. Fatouraie, M., Wooldridge, M., and Wooldridge, S., "In-Cylinder Particulate Matter and Spray Imaging of Ethanol/Gasoline Blends in a Direct Injection Spark Ignition Engine," *SAE Int. J. Fuels Lubr.* 6(1):1-10, 2013, doi:10.4271/2013-01-0259.
18. Ratcliff, M., Windom, B., Fioroni, G., St John, P. et al., "Impact of Ethanol Blending into Gasoline on Aromatic Compound Evaporation and Particle Emissions from a Gasoline Direct Injection Engine," submitted, 2018.
19. Balabin, R., Syunyaiv, R., and Karpov, S., "Molar Enthalpy of Vaporization of Ethanol-Gasoline Mixtures and Their Colloidal State," *Fuel* 86:323-327, 2007, doi:10.1016/j.fuel.2006.08.008.

20. Kar, K., Last, T., Haywood, C., and Raine, R., "Measurement of Vapor Pressures and Enthalpies of Vaporization of Gasoline and Ethanol Blends and Their Effects on Mixture Preparation in an SI Engine," *SAE Int. J. Fuels Lubr.* 1(1):132-144, 2009, doi:10.4271/2008-01-0317.
21. Fioroni, G., Fouts, L., Christensen, E., Anderson, J. et al., "Measurement of Heat of Vaporization for Research Gasolines and Ethanol Blends by DSC/TGA," *Energy Fuels*, 2018 https://pubs.acs.org/doi/10.1021/acs.energyfuels.8b03369.
22. Cannella, W., Foster, M., Gunter, G., and Leppard, W., "FACE Gasolines and Blends with Ethanol: Detailed Characterization of Physical and Chemical Properties," Coordinating Research Council, Alpharetta, GA, CRC report No. AVFL-24, 2014, https://crcao.org/reports/recentstudies2014/AVFL-24/AVFL-24%20FACE%20Gasolines%20Report%20-%20071414.pdf.
23. Fatouraie, M., Frommherz, M., Mosburger, M., Chapman, E. et al., "Investigation of the Impact of Fuel Properties on Particulate Number Emission of a Modern Gasoline Direct Injection Engine," SAE Technical Paper 2018-01-0358, 2018, doi:10.4271/2018-01-0358.
24. Yao, C., Dou, Z., Wang, B., Liu, M. et al., "Experimental Study of the Effect of Heavy Aromatics on the Characteristics of Combustion and Ultrafine Particle in DISI Engine," *Fuel* 203:290-297, 2017, doi:10.1016/j.fuel.2017.04.080.
25. French, R. and Malone, P., "Phase Equilibria of Ethanol Fuel Blends," *Fluid Phase Equilibria* 228-229:27-40, 2005, doi:10.1016/j.fluid.2004.09.012.
26. Dean, J.A. and Lange, N.A., *Lange's Handbook of Chemistry* Fifteenth Edition (New York, NY: McGraw Hill, 1999).
27. Haynes, W.M., *CRC Handbook of Chemistry and Physics: A Ready-Reference Book of Chemical and Physical Data* Ninty First Edition (Boca Raton, FL: CRC Press, 2009).
28. Horsley, L.H., *Azeotropic Data-III* First Edition (Washington, DC: American Chemical Socisty, 1973).
29. Burke, S., Rhoads, R., Ratcliff, M., McCormick, R. et al., "Measured and Predicted Vapor Liquid Equilibrium of Ethanol-Gasoline Fuels with Insight on the Influence of Azeotrope Interactions on Aromatic Species Enrichment and Particulate Matter Formation in Spark Ignition Engines," SAE Technical Paper 2018-01-0361, 2018, doi:10.4271/2018-01-0361.
30. Burke, S., Ratcliff, M., McCormick, R., Rhoads, R. et al., "Distillation-Based Droplet Modeling of Non-Ideal Oxygenated Gasoline Blends: Investigating the Role of Droplet Evaporation on PM Emissions," *SAE Int. J. Fuels Lubr.* 10(1):69-81, 2017, doi:10.4271/2017-01-0581.
31. Sauerbrunn, S. and Zemo, M., "Measuring the Heat of Evaporation by TGA-DSC," https://www.americanlaboratory.com/914-Application-Notes/644-Measuring-the-Heat-of-Evaporation-by-TGA-DSC/, accessed on 20 January 2018.

Contact Information

Gina Fioroni,
gina.fioroni@nrel.gov

Acknowledgments

This research was conducted as part of the Co-Optimization of Fuels & Engines (Co-Optima) project sponsored by the U.S. Department of Energy - Office of Energy Efficiency and Renewable Energy, Bioenergy Technologies and Vehicle Technologies Offices. Co-Optima is a collaborative project of several national laboratories initiated to simultaneously accelerate the introduction of affordable, scalable, and sustainable biofuels and high-efficiency, low-emission vehicle engines. Work at the National Renewable Energy Laboratory was performed under Contract No. DE347AC36-99GO10337. The views expressed in the article do not necessarily represent the views of the U.S. Department of Energy or the U.S. Government. The U.S. Government retains and the publisher, by accepting the article for publication, acknowledges that the U.S. Government retains a nonexclusive, paid-up, irrevocable, worldwide license to publish or reproduce the published form of this work, or allow others to do so, for U.S. Government purposes.

Definitions/Abbreviations

ASTM - ASTM International
Axx - alcohol blend containing xx volume percent alcohol
CBOB - conventional blendstock for oxygenate blending
DHA - detailed hydrocarbon analysis
DI - direct injection
DSC - differential scanning calorimetry
Exx - ethanol blend containing xx volume percent alcohol
FACE - Fuels for Advanced Combustion Engines
HOV - heat of vaporization
MS - mass spectrometry
PM - particulate matter
RBOB - reformulated blendstock for oxygenate blending
RVP - Reid vapor pressure
SI - spark ignition
TGA - thermogravimetric analysis
TIC - total ion current
vol.-% - volume percent

Appendix

TABLE A.1 Blend level validation results for CBOB-alcohol and RBOB-alcohol blends

	Blend Level Measured by Gas Chromatography		
Compound (vol.-%)	10%	20%	30%
RBOB blends			
Methanol	9.7	21.0	31.6
Ethanol	10.1	21.0	31.2
1-Propanol	10.2	20.6	30.9
Isopropanol	10.0	20.4	30.4
2-Butanol	11.3	21.1	30.7
Isobutanol	10.0	20.2	31.6
CBOB blends			
Ethanol	11.1	21.6	32.0
1-Propanol	10.7	21.7	32.2
Isopropanol	10.4	21.2	31.8
2-Butanol	10.8	21.7	32.0
Isobutanol	10.7	21.6	32.3

Created by the National Renewable Energy Laboratory

TABLE A.2 Mass spectrum ions monitored and compound ID

Alcohol	Ion Monitored
2-Butanol	45
Ethanol	45
Isobutanol	42
Isopropanol	45
Methanol	31
1-Propanol	31

Created by the National Renewable Energy Laboratory

TABLE A.3 RVP and total HOV data for alcohol blends with CBOB and RBOB

	RVP (psi)			HOV (kJ/kg)		
Compound (vol.-%)	10%	20%	30%	10%	20%	30%
RBOB	5.28			359		
2-Butanol in RBOB	5.19	4.94	4.73	384	405	426
Ethanol in RBOB	6.44	6.33	6.24	416	478	536
Isobutanol in RBOB	5.20	4.90	4.72	384	409	436
Isopropanol in RBOB	5.73	5.65	5.49	394	430	465
1-Propanol in RBOB	5.37	5.19	4.97	398	439	479
CBOB	11.61			358		
2-Butanol in CBOB	11.68	11.18	10.56	381	406	428
Ethanol in CBOB	13.06	12.67	12.24	420	480	539
Isobutanol in CBOB	11.66	11.18	10.61	384	411	438
Isopropanol in CBOB	12.48	12.00	11.52	394	432	469
1-Propanol in CBOB	12.24	11.83	11.31	399	442	483

Created by the National Renewable Energy Laboratory

FIGURE A.1 D86 curves for alcohol blends with RBOB and CBOB

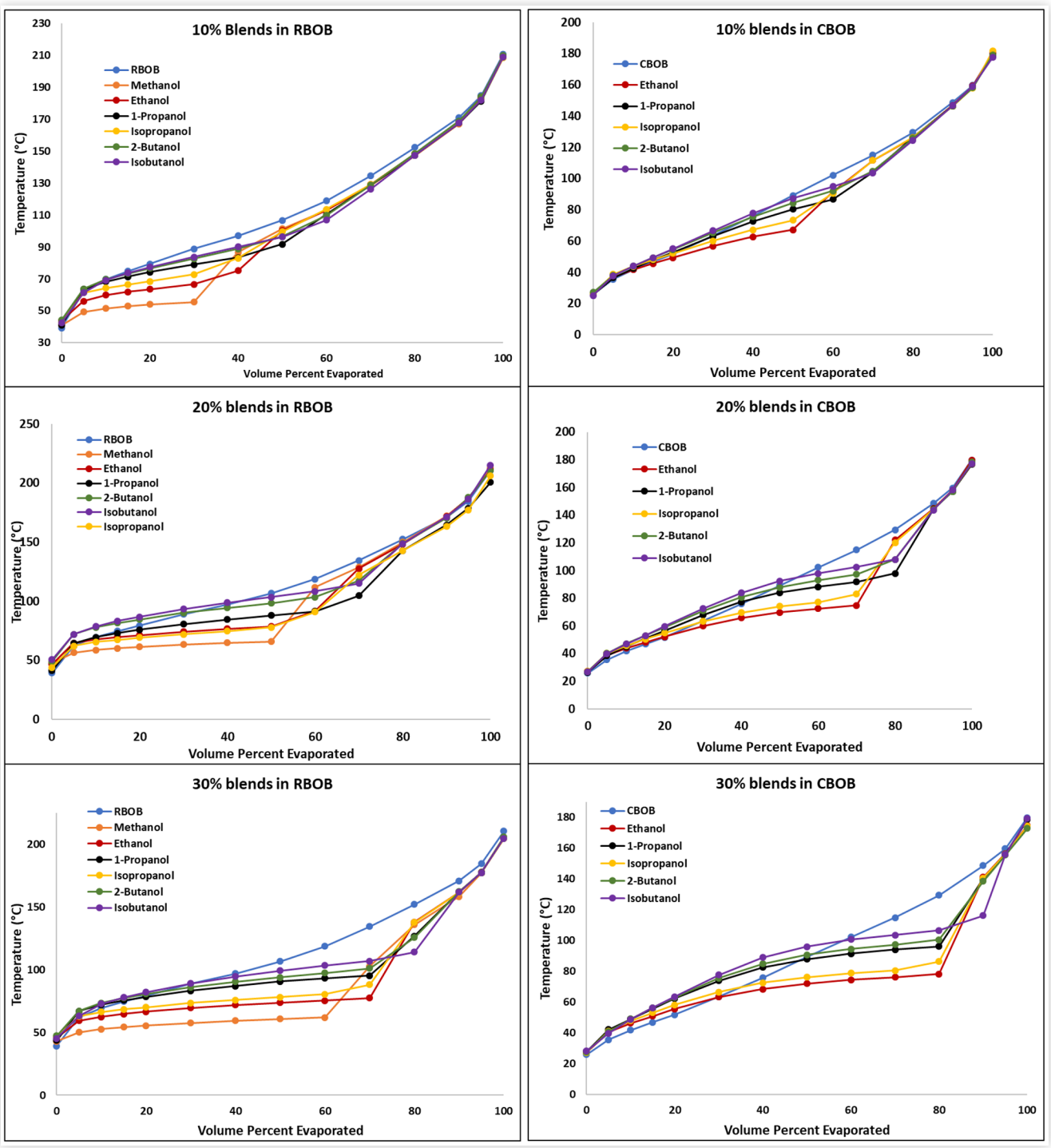

ISSN 0148-7191